

INVESTIGATION OF NONLINEAR SOIL BEHAVIOURS OF REINFORCED CANTILEVER RETAINING WALLS CONSIDERING DIFFERENT BACKFILL SOIL CONDITIONS ACCORDING TO THE EARTHQUAKE LOADS

Şenol GÜRSOY*, Ahmet DURMUŞ**

*Karabük University, Faculty of Fethi Toker Fine Arts and Design, Karabük

**Karadeniz Technical University, Faculty of Engineering, Trabzon

Abstract

Seismic pressures acting on retaining walls are usually estimated using simplified methods but the actual loading on retaining walls during earthquakes is extremely complicated. In this study, it is aimed to present comparatively the seismic analyses of retaining walls considering finite element method (FEM) and analytical methods. A two-dimensional (2D) finite element model is used to analyze the seismic response of retaining wall. A well verified finite element code named LUSAS is utilized for this purpose. The proposed model has mainly the following characteristics: (1) Interface elements are used for backfill soil-wall interaction; (2) The finite element mesh is truncated by using of artificial boundaries to make motion in the vertical direction only at a sufficient distance from the retaining wall. The proposed model is used to study the seismic response of a cantilever retaining wall according to North-South component of the Erzincan earthquake (1992). The finite element model is verified by comparing the results obtained from analytical methods with satisfactory agreement.

Keywords: Analytical methods, Retaining Walls, Seismic analyses, Seismic soil pressure.

1. Introduction

Many authors [1, 2] have reported numerous cases of damage or failure of retaining walls induced by excessive displacement or failure during recent earthquakes. In order to avoid this situation, retaining walls have to be properly designed for the dynamic loading caused by earthquakes. In other words, the structural analysis and stabilization check of retaining walls should be performed in accordance with the earthquake loads as well.

Conventional design methods usually require estimation the static soil pressure behind a retaining wall and choosing the wall geometry in order to satisfy equilibrium conditions with specified factors of safety. But it is not enough to design soil retaining walls located in earthquake regions by considering only the static pressures. Seismic soil pressures acting on retaining walls are also necessary for designing of these walls. The behavior of retaining walls during earthquakes is considered as an important design problem in seismic regions. The most retaining walls use it own mass for stability against failures. It is clear that it is necessary to determinate soil pressures properly and exactly in order to decrease the damages to emerge on retaining walls because of seismic soil pressures. Understanding of the behavior of retaining walls requires consideration of the mass and stiffness of the wall, the backfill soil properties and the interaction among them.

In this paper, the behavior of reinforced concrete cantilever retaining walls is investigated comparatively by using different analytical methods and structural analysis program LUSAS [3] which uses the finite element method, according to North-South component of 1992 Erzincan earthquake. The proposed model is verified by comparing its predictions to results from analytical methods. Thus, in this research is to give specific guidance for the analysis and design of earthquake resistant retaining walls.

2. Background Regarding Seismic Soil Pressures and Design of Retaining Walls

It is known that the seismic soil pressures acting on the retaining walls in the earthquake regions are different from the static soil pressures as distribution and magnitude. Determining the seismic soil pressures acting on retaining walls due to earthquakes requires very complicated calculations. That's why; determining the mentioned pressures generally uses pseudo static methods.

The seismic analysis of retaining walls has generally been based on a pseudo-static method known as Mononobe-Okabe method which was developed with extension of Coulomb's equilibrium [4, 5, 6]. Afterwards great deals of research works have been performed to evaluate and improve it [7, 8, 9, 10, 11]. Some well known analytical methods used in determining dynamic pressure acting on retaining walls during the earthquakes are given in Table 1.

Table 1. Some analytical methods used in calculating seismic soil pressure acting on retaining walls

Method	Total active soil pressure coefficient (K_{at}) and Application points (h)	Total active lateral soil thrust (P_{at})
Mononobe-Okabe Method	$K_{at} = \frac{\cos^2(\varphi - \alpha - \lambda)}{\cos \lambda \cdot \cos^2 \alpha \cdot \cos(\delta + \alpha + \lambda) \cdot \left[1 + \sqrt{\frac{\sin(\delta + \varphi) \cdot \sin(\varphi - i - \lambda)}{\cos(\delta + \alpha + \lambda) \cdot \cos(i - \alpha)}} \right]^2}$ <p>(where $k_h = a_h / g$, $k_v = a_v / g$, $\lambda = \tan^{-1}[k_h / (1 - k_v)]$ $h = H/3$)</p>	$P_{at} = \frac{1}{2} \cdot K_{at} \cdot \gamma \cdot H^2 \cdot (1 - k_v)$
Steedman-Zeng Method	$K_{at} = \frac{\sin(\theta - \varphi)}{\tan \theta \cdot \cos(\delta + \varphi - \theta)} + \frac{k_h \cdot \cos(\theta - \varphi)}{\tan \theta \cdot \cos(\delta + \varphi - \theta)} \cdot \sin \left[\omega \left(t - \frac{z}{V_s} \right) \right]$ $h = H - \frac{2\pi^2 \cdot H^2 \cdot \cos \omega \cdot \xi + 2\pi \lambda_o \cdot H \cdot \sin \omega \cdot \xi - \lambda_o^2 \cdot (\cos \omega \cdot \xi - \cos \omega t)}{2\pi \cdot H \cdot \cos \omega \cdot \xi + \pi \cdot \lambda_o (\sin \omega \cdot \xi - \sin \omega t)}$ <p>(where $\lambda_o = 2\pi V_s / \omega$ $\xi = (t - H / V_s)$)</p>	$P_{at} = \frac{Q_h \cdot \cos(\theta - \varphi) + W_d \cdot \sin(\theta - \varphi)}{\cos(\delta + \varphi - \theta)}$
Prakash-Saran Method	$(K_{at})_c = \frac{\cos(\theta_v + \varphi + \alpha) \cdot \sec \alpha + \cos \varphi \cdot \sec \theta_v}{\sin(\theta_v + \varphi + \alpha + \delta)}$ $(K_{at})_q = \frac{[(n + 1) \cdot \tan \alpha + \tan \theta_v] [\cos(\theta_v + \varphi) + k_h \cdot \sin(\theta_v + \varphi)]}{\sin(\theta_v + \varphi + \alpha + \delta)}$ $(K_{at})_\gamma = \frac{[(n + 1) \cdot (\tan \alpha + \tan \theta_v) + n^2 \cdot \tan \alpha] [\cos(\theta_v + \varphi) + k_h \cdot \sin(\theta_v + \varphi)]}{\sin(\theta_v + \varphi + \alpha + \delta)}$ $h = \frac{P_{as} \cdot H / 3 + P_{ad} \cdot (0,5H)}{P_{at}} \quad (\text{where } n = \frac{h_o}{H_1})$	$P_{at} = \frac{\gamma \cdot H^2}{2} \cdot (K_{at})_\gamma + q \cdot H \cdot (K_{at})_q - c \cdot H \cdot (K_{at})_c$
Seed-Whitman Method	$K_{at} = K_{as} + 0,75 \cdot k_h$ $h = \frac{P_{as} \cdot H / 3 + P_{ad} \cdot (0,6H)}{P_{at}}$	$P_{at} = \frac{1}{2} \cdot K_{at} \cdot \gamma \cdot H^2 \cdot (1 - k_v)$

Requirements related to retaining walls with different analytical methods are compared by Gürsoy and Durmuş [12]. Also, some of studies have been performed to concern with retaining wall-soil interaction [13, 14, 15, 16, 17].

3. General Description of the Code LUSAS

The technique of finite element analysis (FEA) lies in the development of a suitable mesh arrangement. The mesh discretisation must offset the need for a fine mesh to give an accurate stress distribution and reasonable analysis time. On the other hand, solution control parameters before running the analysis, important “control” parameters were required as input to define and adjust the algorithm during the solution process. These parameters were specified to define the convergence criteria, initial load factor, and load increment for each of the analysis cases. Load increment was applied with an initial load factor of 1.0. The Newton-Raphson iteration method was used to achieve equilibrium between the load increment applied and the internal nodal forces produced in the structure. The convergence criteria used in the iteration process was based on the sum of the squares of all the residual forces, normalized by the sum of the squares of all the external forces. In this analysis, a load criterion set at 1% produced an acceptable balance between solution performance and numerical accuracy.

3.1. Material Model Used for the Soil Elements

LUSAS incorporates a choice of several constitutive models to represent the behavior of soil. These models range from linear elastic to nonlinear elasto-plastic ones. Models consist of quadrilateral isoparametric element with four degrees of freedom for 2D plane strain problem. Also, interface behavior can be modeled in LUSAS [18] using joint element.

3.1.1. Basic equations for the soil elements

The soils (different type backfills in this study) are modeled using four-node isoparametric plane strain quadrilateral element. Basic formulation for soil-structure interaction using finite element method with Langrangian approach is summarized below:

1. Soil is compressible. The used finite element is based on a formulation in which the soil strains are calculated from the linear strain-displacement equations. The only strain energy considered is associated with the compressibility of the soil.
2. Displacement field is constrained to be irrotational by introduction of a rotational stiffness.

Two dimensional isoperimetric soil elements with four nodes are considered in Langrangian approach. Global (x, y) and local axes (r, s) are given in Figure 1 for this element.

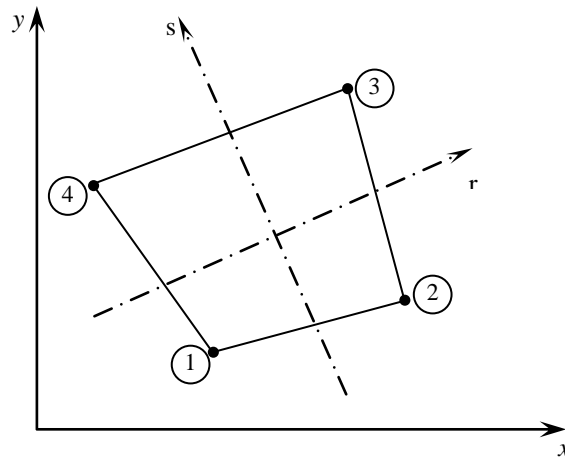


Figure 1. Two dimensional isoperimetric soil elements considered

Expressions for mass and rigidity matrices are given below;

$$K = \int_v B^T . E . B . dV \rightarrow K = \sum_i \sum_j \eta_i . \eta_j . B_{ij}^T . E . B_{ij} . \det J_{ij} \tag{1}$$

$$M = \rho \cdot \int_v N^T . N . dV \rightarrow M = \rho \sum_i \sum_j \eta_i . \eta_j . N_{ij}^T . N_{ij} . \det J_{ij} \tag{2}$$

where J is the Jacobean matrix, N_{ij} is the interpolation function, η_i and η_j are weighting functions, ρ is the

mass density of soil, B is the strain-displacement matrix which is obtained from $\epsilon = \mathbf{B} \cdot \mathbf{u}$ expression. After the mass and rigidity matrices are obtained by Eqs. (1) and (2), total potential and kinetic energy expressions in the finite element can be written as;

$$U = \frac{1}{2} \cdot \mathbf{u}^T \cdot \mathbf{K} \cdot \mathbf{u} \quad (3)$$

$$T = \frac{1}{2} \cdot \mathbf{v}^T \cdot \mathbf{M} \cdot \mathbf{v} \quad (4)$$

If the expressions for kinetic and potential energies are substituted into Lagrange equation, which is

$$\frac{d}{dt} \left(\frac{\partial T}{\partial \dot{u}_j} \right) - \frac{\partial T}{\partial u_j} + \frac{\partial U}{\partial u_j} = F_j \quad (5)$$

where u_j is the j^{th} displacement component and F_j is the applied external load, the governing equation can be written as:

$$\mathbf{M} \cdot \ddot{\mathbf{u}} + \mathbf{K} \cdot \mathbf{u} = \mathbf{R} \quad (6)$$

where $\ddot{\mathbf{u}}$ is the acceleration and R is a general time varying load vector

3.1.2. An elasto-plastic model based on Drucker-Prager failure criterion

Drucker-Prager elasto-plastic failure criterion is generally used for soil element [19, 20]. In this study, nonlinear behavior of the backfill soils are expressed with Drucker-Prager failure criterion (Figure 2) and failure surface (f) is calculated as follows;

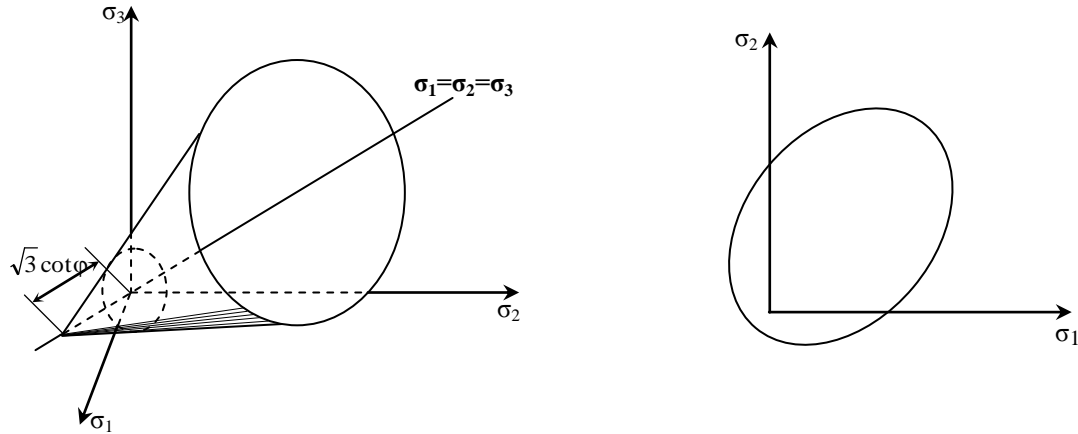


Figure 2. Drucker-Prager schematic failure surfaces at two dimensional principal stress planes and at three dimensional principal stress spaces

$$f(I_1, J_2) = \mu \cdot I_1 + \sqrt{J_2} - k = 0 \quad (7)$$

where I_1 shows the first invariant of stress tensor (σ_{ij}), J_2 the second invariant concerning the deviation of this tensor (S_{ij}). μ and k are obtained from equations below;

$$\mu = \frac{2 \cdot \sin \varphi}{\sqrt{3} \cdot (3 - \sin \varphi)} \quad k = \frac{6 \cdot c \cdot \cos \varphi}{\sqrt{3} \cdot (3 - \sin \varphi)} \quad (8)$$

where c is soil cohesion and φ is angle of soil internal friction. For elasto-plastic materials, the general stress-

strain relationships can be written as follows:

$$d\sigma_{ij} = D_{ijkl}^{ep} \cdot d\varepsilon_{kl} \quad (9)$$

where D_{ijkl}^{ep} is elasto-plastic material matrix and consist of component as follows:

$$D_{ijkl}^{ep} = \underbrace{2G\delta_{ik}\delta_{jl} + (K - \frac{2}{3}G)\delta_{ij}\delta_{kl}}_{D^e} - \underbrace{\frac{1}{H}H_{ij}H_{kl}}_{D^p} \quad (10)$$

where H and H_{ij} can are written as follows, respectively:

$$H = 9K\alpha^2 + G \quad (11)$$

and

$$H_{ij} = 3K\alpha\delta_{ij} + G/\sqrt{J_2} \quad (12)$$

where K and G are bulk and shear modules of soil material, respectively.

Drucker-Prager failure criterion was incorporated into the program LUSAS as two and three dimensional. Two dimensional model used in this study is available in the reference [20]. In the elasto-plastic model, it is accepted that stresses and strains in the element are σ_{ij}^n and ε_{ij}^n at the end of the n^{th} loading increment, respectively.

3.2. Joint Interface Model

The interface model for the connection between the retaining wall and the backfill soil is used in the analysis, which is available in the LUSAS code [18]. This model was called “Joint” element, which contains transitional springs. The model is available in plane stress and plane strain elements, a line of which must lie between the two discrete 2D bodies in the finite element mesh.

Although it is possible to use joint elements for three-dimensional analysis, the present study is concerned with two-dimensional plane-strain conditions. Joint elements in this study called JNT3 which are used to model the interface between the retaining wall and the backfill soil. These 2D joint elements which connect two nodes by two springs in the local x and y-directions are described. Such elements are suitable for static and dynamic when substitutes part of horizontal joint. Also, mass and the geometric thicknesses of the joint elements are zero.

3.3. Nonlinear Incremental-Iterative Procedure

In the present analysis, Newton-Raphson method has been used for solving the nonlinear equations involved in a plasticity analysis. In this method the load is applied in increments, and the stiffness matrix in the each iteration is updated. After each iteration, the step portion of the total loading which is not balanced is calculated and used in the next step to compute an additional increment of displace. The solution is said to be converged in the equilibrium after a number of iterations when the restoring force equals to the applied loads (or at least to within some tolerance). The details of full Newton-Rahpson method are discussed by LUSAS [3].

4. Numerical Example

In this article, the dimensions and properties of retaining wall and different backfill soil parameters considering for numerical application are shown in Figure 3. Besides, passive thrust is neglected in the analyses and stability controls. In the example, given the Young’s modulus, Poisson ratio and unit weight of retaining wall are taken to be $E_c = 2,85 \times 10^7 \text{ kN/m}^2$, $\nu_c = 0.2$ and $\gamma_c = 25 \text{ kN/m}^3$, respectively.

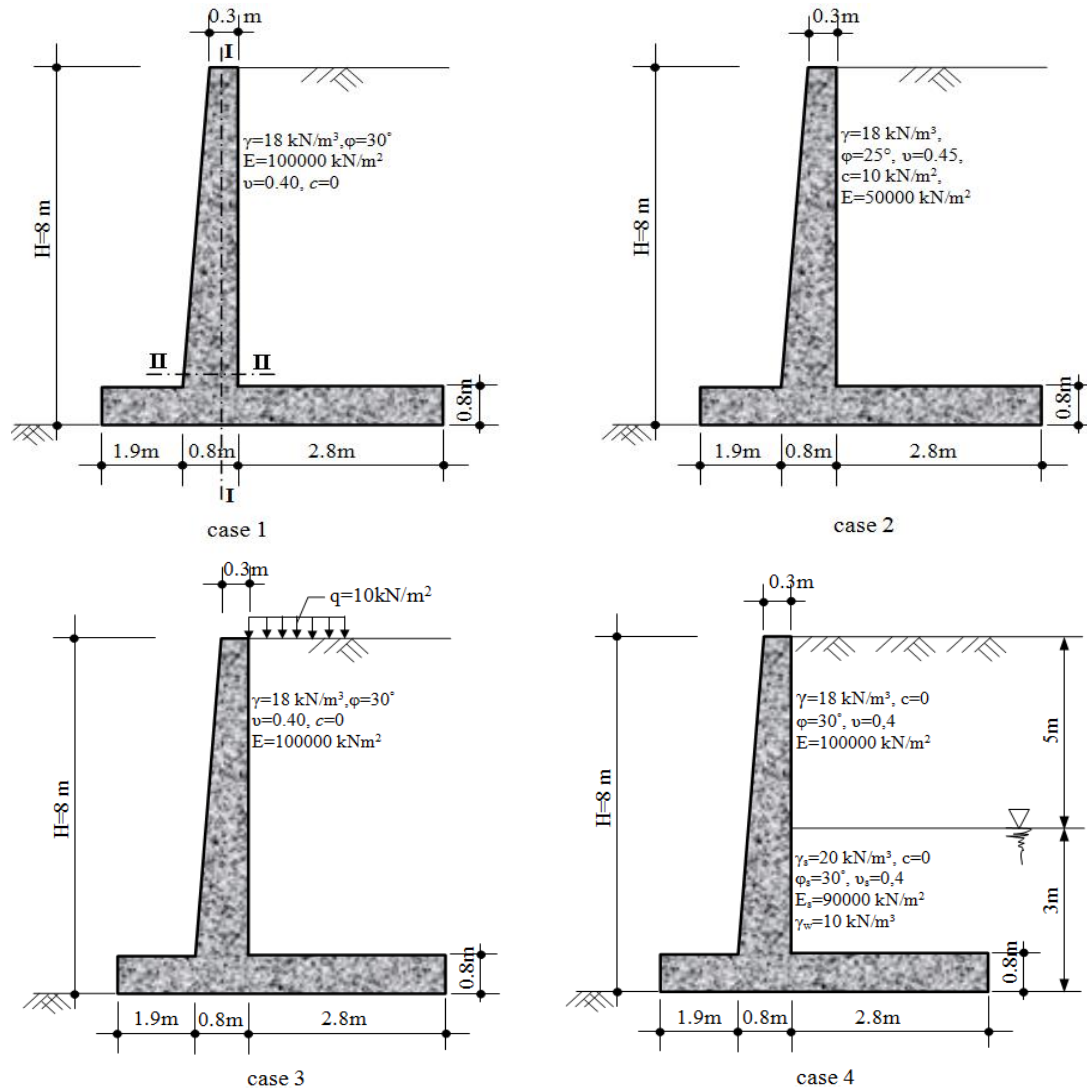


Figure 3. Example for retaining wall and soil parameters

The proposed model is used to carry out a study on the seismic response of an 8m high reinforced cantilever retaining wall. The retaining wall retains different backfill soils and has fixed foundation of the same, too. In order to choose the proper wall width (for all case) the traditional approach is used with an acceleration coefficient equal to 0,16 ($k_h=0.16$).

Figure 4 shows the finite element modeling of the cantilever retaining wall. In the proposed model, element dimensions are reduced until they not have in significant effect on the results of analyses. Small elements are used especially for the soil models close to the retaining wall on which stress and strains are of very importance. Finite element analysis is carried out with LUSAS V15.7 (3) plane strains condition. Damping ratio in the all analyses is taken as 5%. The proposed model for the dynamic response of cantilever retaining wall can be summarized as follows:

1. Both the wall and the backfill soil elements (different backfill soils in this study) are modeled by a 2D-four nodes quadrilateral isoparametric finite element. Also, the backfill soil material is modeled using the Drucker-Prager failure criteria, too. This model consists of a failure surface (Figure 2).
2. Interface elements (joint elements) are used between the soil and the wall (at the back face of the wall).
3. The optimum mesh length is found to be about 40m, which corresponds to truncating the mesh at about 5H distance from the retaining wall [21].
4. The finite element mesh length is truncated by using vertical direction motion boundaries at sufficient distance from the retaining wall and the wall and backfill soil is supported rigidly from the base.

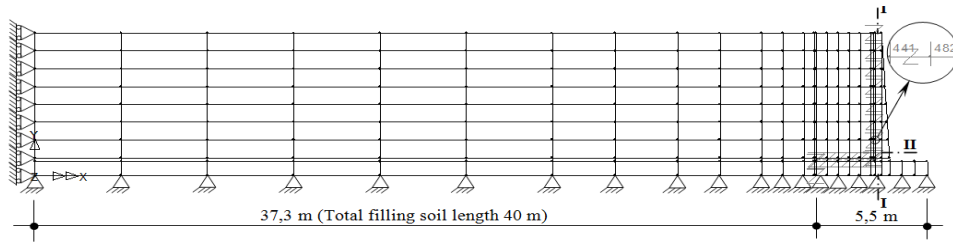


Figure 4. Finite element mesh used in the analyses of the retaining wall

Reinforced cantilever retaining wall are subject to the first 10s' part (Figure 5) of North-South component of the March 13, 1992 Erzincan earthquake in Turkey.

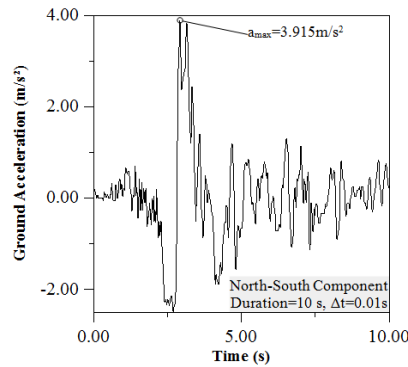


Figure 5. Ground acceleration of North-South component of Erzincan earthquake

Maximum total (static+dynamic) active soil pressure distributions obtained from the linear elastic and elasto-plastic (Drucker-Prager) analyses carried out in the time domain for the different backfill soils are given in Figure 6 together with the ones calculated by the aid of different analytical methods.

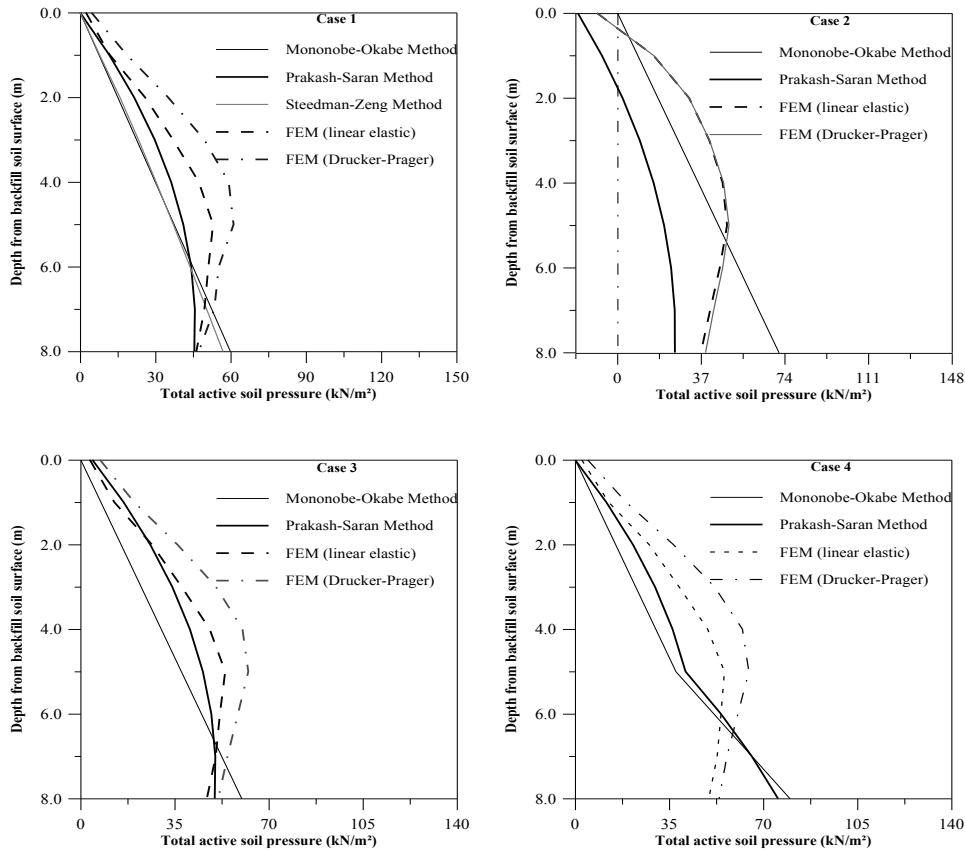


Figure 6. Maximum total active soil pressure distributions acting on the retaining wall according to different methods

As it is seen from these figures, total active soil pressure obtained according to Mononobe-Okabe method continuously increase from the surface of the soil to the wall base. Also, maximum total active pressure distribution obtained considered Drucker-Prager elasto-plastic failure criterion of the backfill soil according to the proposed model (FEM) are generally greater than the ones obtained from analytical method and linear elastic assumption. However, in the part near to the wall base it has smaller values according to Mononobe-Okabe method. On the other hand, in the case of clayey soil-backfill (case 2), maximum total active soil pressure distributions obtained from the FEM elasto-plastic analysis generally coincide with the distributions obtained from the linear elastic analysis. This situation reveals the importance of backfill soil type in the designs of retaining walls.

Total active soil pressures variation occurred throughout the earthquake process at the node point 482, where active soil pressures is maximum, according to the proposed model for the different backfill soils given in Figure 7.

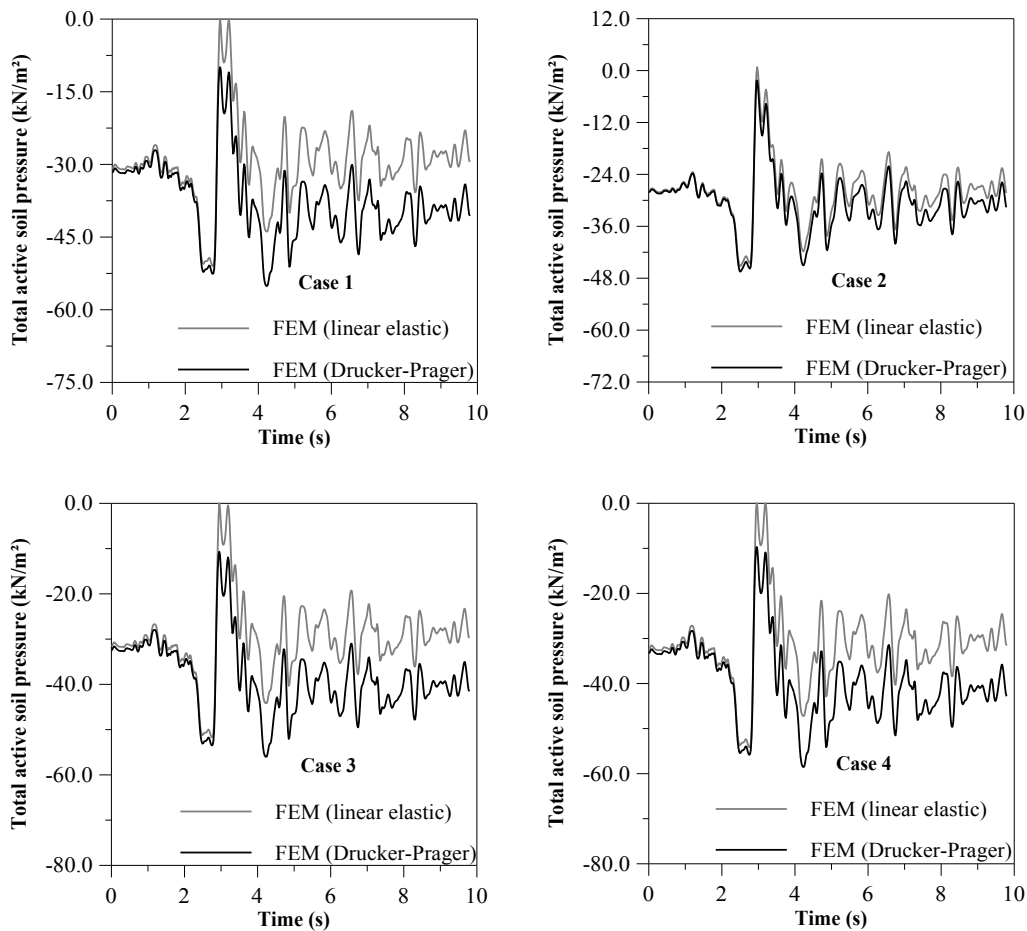


Figure 7. Time history of total active soil pressure in 482 node point of the retaining wall from linear and nonlinear analyses for different backfill soils according to FEM

From these figures, total active soil pressures variation obtained from the analyses related to elasto-plastic (nonlinear) behavior of backfill soils are greater than the ones obtained from the elastic (linear) analyses. However, total active soil pressure variation obtained from the elasto-plastic analysis for case 2 (the clay backfill soil) generally coincides with the variation obtained from the elastic (linear) analysis. Also, one can easily infer that amplitudes of pressures increase between 2s-5s and total active soil pressures variation occurring during the earthquake at this node point (482) is similar to earthquake acceleration given in Figure 5.

The maximum values of horizontal and vertical stresses, in I-I and II-II sections, obtained along wall depth from nonlinear analysis according to Drucker-Prager failure criterion for different backfill by means of the proposed model are given Figure 8-11. It can be observed from Figure 8-11 that case 3 and case 4 always yield the largest response. Also stress values obtained from the case 2 is smaller than the other cases.

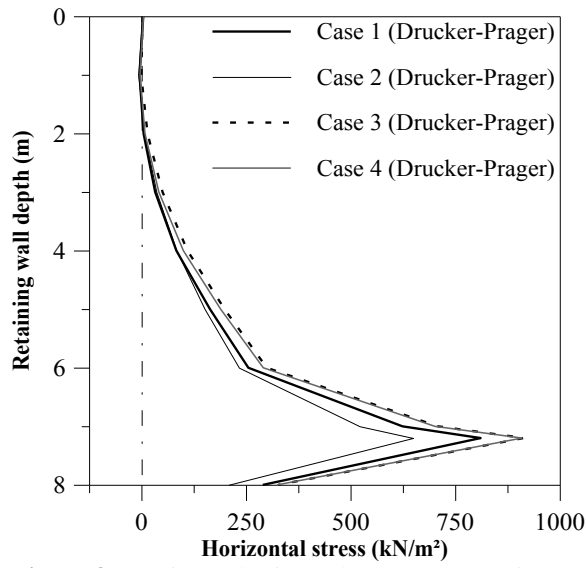


Figure 8. Maximum horizontal stresses on section I-I

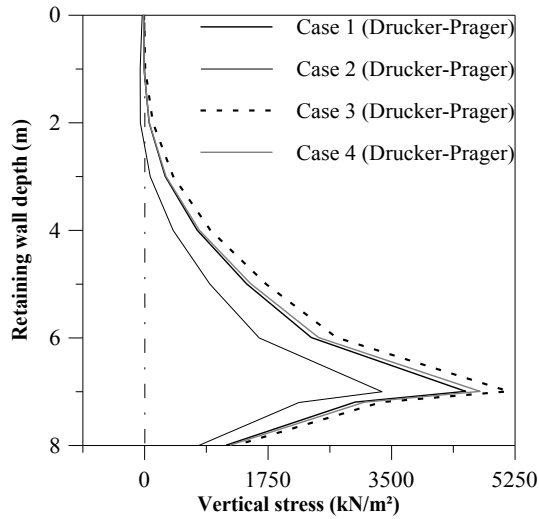


Figure 9. Maximum vertical stresses on section I-I

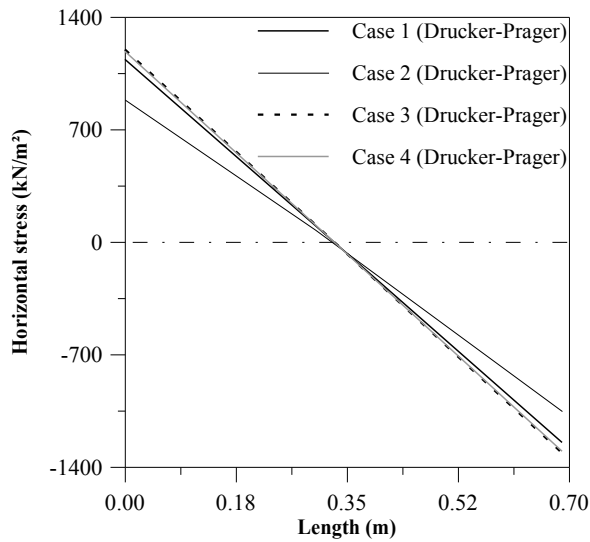


Figure 10. Maximum horizontal stresses on section II-II

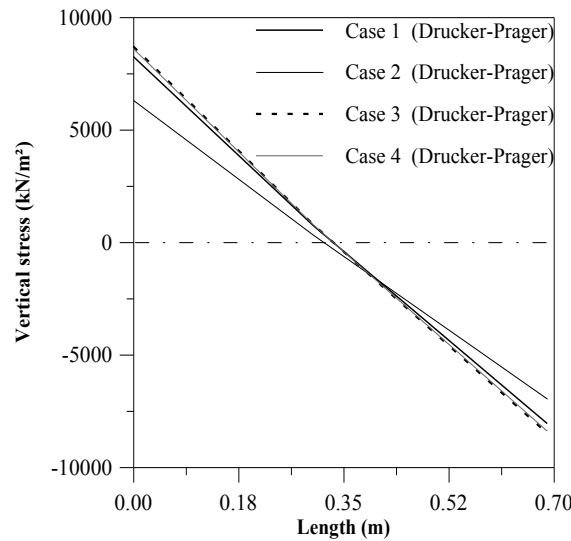


Figure 11. Maximum vertical stresses on section II-II

Maximum total active soil thrust, application point and overturning moment values acting on the retaining wall according to Mononobe-Okabe, Steedman-Zeng, Prakash-Saran, Seed-Whitman and finite element methods for the different backfill soils are given in Table 2.

Table 2. The total active soil thrust, application point and overturning moments calculated according to different methods

Used Method		The total active soil thrust (kN)	Application point (m)	Overturning moment (kNm)
Mononobe-Okabe Method	Case 1	239.35	2.667	638.346
	Case 2	285.596	2.667	761.684
	Case 3	239.35	2.667	638.346
	Case 4	269.399	2.481	668.379
Steedman-Zeng Method	Case 1	253.82	3.35	850.297
	Case 2	303.131	3.245	983.66
	Case 3	253.82	3.35	850.297
	Case 4	298.823	2.996	895.274
Prakash-Saran Method	Case 1	253.82	3.045	772.88
	Case 2	95.997	3.559	341.653
	Case 3	289.1	3.161	913.845
	Case 4	298.82	2.74	818.77
Seed-Whitman Method	Case 1	261.12	3.231	843.7
	Case 2	302.89	3.154	955.31
	Case 3	261.12	3.231	843.7
	Case 4	306.12	2.903	888.7
Finite element Method	Case 1	linear	-	838.043
		nonlinear	-	1054.387
	Case 2	linear	-	782.592
		nonlinear	-	803.982
	Case 3	linear	-	860.562
		nonlinear	-	1097.957
	Case 4	linear	-	873.991
		nonlinear	-	1103.837

As it can be seen from this table, that for all cases the overturning moment value calculated from the elasto-plastic analyses by proposed model (FEM) are greater than the ones calculated for the others. This situation refers that the walls designed according to linear assumption with the finite element method or these with the analytical methods may remain unsafe. Thus, this fact reveals the importance of considering nonlinear (elasto-plastic) effects of retaining walls in case of an earthquake.

Horizontal displacement distributions obtained along wall depth from the nonlinear (elasto-plastic) analyses for different backfills with proposed model are given Figure 12. From this figure, displacement in the crest point of the retaining wall in case 3 is greater than those of other cases. This finding showed that in cases of having surcharge load and saturated backfill soil, the vibration period of the retaining wall increases and this is important for design of retaining walls of backfill soil type.

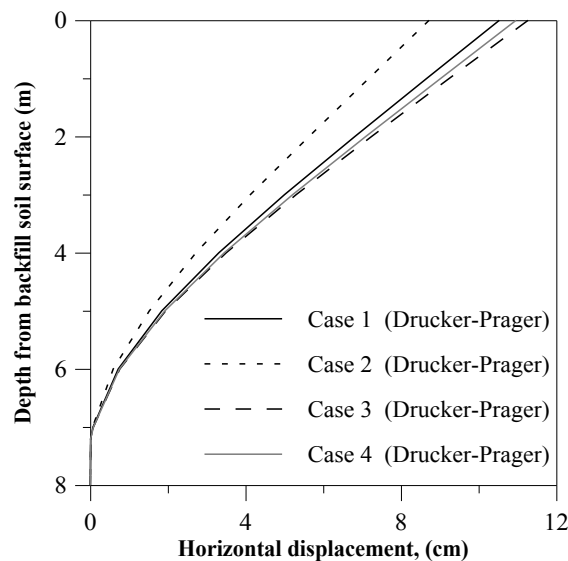


Figure 12 Maximum horizontal displacements of the retaining wall obtained from nonlinear analysis for different backfill soils according to the proposed model

5. Conclusions and Recommendations

In this paper, the effect of the backfill soil characteristics on the seismic response of retaining wall-backfill soil systems subjected to earthquake is investigated by using the finite element method and the relative earthquake performance presented comparison with the analytical methods. On the basis of the current study, the main conclusions are given as follow:

1. Overturning moment values obtained from the nonlinear (elasto-plastic) analysis with finite element method according to proposed model of retaining wall are greater than the ones obtained from linear analysis and analytical methods. This situation requires to consideration of nonlinear soil behavior in designs of retaining walls.
2. The variation of during earthquake of the total active soil pressures obtained from linear and nonlinear analyses in the time domain of the retaining wall is similar to variation of ground motion acceleration. Also, the total active soil pressures obtained from nonlinear analyses are greater than the ones linear analyses. In this situation, determined cross-section dimensions and the stability control done with the results obtained from linear analyses are not able to provide the results of nonlinear analyses.
3. From the solutions carried out for different backfill soils; retaining wall displacements, stresses, total active soil pressures and overturning moments change according to backfill soil. Hence, this shows that for a safe and economical design the effect of backfill soil type should be considered.
4. Overturning moment values obtained from linear analyses the carried out by proposed model are approximately same to the values obtained from the analytical methods.
5. Outcome of the all the analyzed cases provided that the results obtained from the elastic (linear) analysis according to case 2 are in good agreement with those of elasto-plastic (nonlinear) analysis. This conclusion showed that the backfill soil does not yield.

6. It is generally observed that the maximum total active soil pressure distributions calculated by proposed model are greater than those of the analytical methods.

7. To generalize these results from the different type backfill soils, solutions must be obtained using many earthquake inputs and foundation models. Results obtained from different inputs and models must be evaluated against each other.

Notation

a_h	: Horizontal ground acceleration
a_v	: Vertical ground acceleration
c	= Soil cohesion
E	= Young's modulus of backfill soil
E_s	= Young's modulus of saturated backfill soil
H	= Height of retaining wall
H_1	= Height of retaining wall free from crack
h	= Application point of total active soil thrust from the wall base
h_o	= The cracked zones in clay soils
i	= Angle of backfill soil slope
K_{as}	= Static active soil pressure coefficient
K_{at}	= Total active soil pressure coefficient
k_h	= Horizontal seismic coefficient
k_v	= Vertical seismic coefficient
P_{ad}	= Dynamic active lateral soil thrust per unit length
P_{as}	= Static active lateral soil thrust per unit length
P_{at}	= Total active lateral soil thrust per unit length
q	= Surcharge loading
Q_h	= The total inertial forces acting on the retaining wall
W_d	= Soil wedge weight
V_s	: Velocity of shear wave
α	= Angle of the wall back surface to vertical
γ_b	: Buoyant unit weight of soil
γ	= Unit weight of soil
γ_s	= Saturated unit weight of soil
γ_w	= Unit weight of water
δ	= Friction angle between the wall and backfill soil
θ	= Angle of the soil wedge to horizontal
θ_v	= Angle of the soil wedge to vertical
ν	= Poisson ratio of backfill soil
ν_s	= Poisson ratio of saturated backfill soil
ϕ	= Angle of soil friction
ϕ_s	= Angle of saturated soil friction
ω	= Angular velocity

References

1. Durmuş, A., Gürsoy, Ş., Angın, Z., Doğangün, A., Analysis of retaining walls under earthquake effect. 8th Soil Mechanics and Foundation Engineering National Congress, İstanbul 2000, 331-340. (in Turkish)
2. Nazarian, H., Hadjian, A.H., Earthquake Induced Lateral Soil Pressure on Structures, J. Geotechnical Eng., ASCE 1979, 105 (GT9).
3. LUSAS, (2006a) "Lusas User and Theory Manuals", Versions 13.7-6, FEA Ltd, Kingston upon Thames.
4. Mononobe, N., Consideration into Earthquake Vibrations and Vibration Theories, J Japan Soc Civil Eng, 1924, 10 (5): 1063-1094.
5. Okabe, S., General Theory of on Earth Pressures on Seismic Stability of Retaining Wall and Dam, J Japan Soc Civil Eng, 1924, 10(5), 1277-1323.
6. Mononobe, N., Matsuo, H., On the determination of earth pressures during earthquakes. 9th Proceeding World Engineering Congress, Tokyo 1929: 177-185.
7. Prakash, S., Saran, S., Static and dynamic earth pressures behind retaining walls. Proceeding of the 3rd Symposium on Earthquake Engineering, India 1966, 1: 277-288.

8. Seed, H.B., Whitman, R.V., Design of earth retaining structures for dynamic loads. ASCE Special Conference Lateral Stresses in the Ground and Design of Earth Retaining Structures, Cornell 1970: 103-147.
9. Richard, R.J., Elms, D., Seismic Behavior of Gravity Retaining Walls, Journal of Geotechnical Engineering, ASCE, 1979, 105: 449-464.
10. Whitman, R.V., Liao, S., Seismic design of gravity retaining walls. Proc 8th World Conference on Earthquake, San Francisco 1984, 3: 533-540.
11. Steedman, R.S., Zeng, X., The seismic response of waterfront retaining walls, Geotechnical Special Publication-ASCE, New York, 1990, 25: 872-886.
12. Gürsoy, Ş., Durmuş, A., Design according to earthquake of reinforced concrete retaining wall. 6th International Congress on Advances in Civil Eng. (ACE2004), İstanbul 2004; 402-411. (in Turkish)
13. Nadim, F., Whitman, R.V., Couple sliding and tilting of gravity walls during earthquakes. 8th Proceeding World Conference on Earthquake Engineering, San Fransisco 1984, 3: 477-484.
14. Zhao, C., Valliapan, S., Dynamic Analysis of a Reinforced Retaining Walls Using Finite and Infinite Elements Coupled Method, Computers and Structures, 1993, 47(2): 239-244.
15. Steedman, R.S., Seismic soil-structure interaction of rigid and flexible retaining walls. Proceeding of The Second International Conference on Earthquake Geotechnical Engineering, Lisboa, PORTUGAL 1999, 3: 949-956.
16. Woodward, P.K., Griffiths, D.V., Comparison of the Pseudo-Static and Dynamic Behavior of Gravity Retaining Walls, Geotechnical and Geological-Engineering, 1996, 14: 269-290.
17. Gürsoy, Ş., Durmuş, A., Investigation of Linear and Nonlinear of Behaviours of Reinforced Concrete Cantilever Retaining Walls According to the Earthquake Loads Considering Soil-Structures Interactions, Structural Engineering and Mechanics, 2009, 31(1): 75-91.
18. LUSAS, (2006b) "Lusas Element Library", Versions 13.7-6, FEA Ltd, Kingston upon Thames.
19. Drucker, D.C., Prager W., Soil Mechanics and Plastic Analysis of Limit Design, Quart. Applied Mathematics, 1952, 10 (2).
20. Chen, C.P., Mizuna, E., (1990) "Nonlinear Analysis of Soil Mechanics", Elsevier Science Publisher, Amsterdam.
21. Gürsoy, Ş., (2006) "Investigation of linear and nonlinear of behaviours of reinforced concrete retaining walls according to the earthquake loads considering soil-structures interactions", *PhD Thesis*, Black Sea Technical University (KTU), Turkey, (in Turkish).